Unveiling the Dispersion Kernel in DSC-MRI by Means of Dispersion-Compliant Bases and Control Point Interpolation Techniques

Marco Pizzolato, Rutger H.J. Fick, Timothé Boutelier, Rachid Deriche

HAL Id: hal-01408170

https://inria.hal.science/hal-01408170

Submitted on 3 Dec 2016

Unveiling the Dispersion Kernel in DSC-MRI
by Means of Dispersion-Compliant Bases and Control Point Interpolation Techniques

Marco Pizzolato[1][†], Rutger Fick[1], Timothé Boutelier[2], Rachid Deriche[1]

Synopsis. In DSC-MRI the presence of dispersion affects the estimation, via deconvolution, of the residue function that characterizes the perfusion in each voxel. Dispersion is descibed by a Vascular Transport Function (VTF) which knolewdge is essential to recover a dispersion-free residue function. State-of-the-art techniques aim at characterizing the VTF but assume a specific shape for it, which in reality is unknown. We propose to estimate the residue function without assumptions by means of Dispersion-Compliant Bases (DCB). We use these results to find which VTF model better describes the *in vivo* data for each tissue type by means of control point interpolation approaches.

Purpose. To assess *in vivo* which vascular transfer function (VTF) better describes the brain vascular dynamic in DSC-MRI.

Introduction. Dispersion is a physiological phenomenon present in DSC-MRI data and its characterization is fundamental to assess the reliability of hemodynamic parameters while potentially revealing pathological conditions [1]. Dispersion affects the time-dependent residual amount of tracer $R(t)$ calculated for each voxel via deconvolution of the measured arterial $C_a(t)$ and tissular $C_{ts}(t)$ concentrations [2, 3]. Mathematically the computed effective residual amount is computed as the convolution $R^{eff}(t) = R(t) \otimes VTF(t)$, where VTF is the probability density of the transit times t from the arterial measurement location to the voxel where $C_{ts}(t)$ is measured. A recent state-of-the-art technique [4], henceforth CPI+GDK, disentagles the contributions of VTF and $R(t)$ by estimating a set of control points whose interpolation is convolved to a gamma dispersion kernel (GDK) that is assumed as model for the VTF

$$GDK(t) = \frac{s^{1+sp}}{\Gamma(1+sp)} t^{sp} e^{-st} \tag{1}$$

where s, p are unknown. However, the true shape of VTF is unknown, therefore the GDK assumption may not be true.

We propose instead to perfom deconvolution with Dispersion-Compliant Bases [5] (DCB) which make no assumptions on the VTF. We then implement variants of CPI+GDK for the well-known exponential (CPI+EDK) and log-normal (CPI+LNDK) dispersion kernels [4], to see which one, among the three, better describes the DCB results *in vivo*. We finally obtain maps of the brain showing for each voxel what is the dispersion kernel that better describes the data.

Methods. We perform DCB deconvolution on a sampling grid $t_1, t_2, .., t_M$ representing $R(t)$ as [5]

$$R^{eff}_{DCB}(t) = \Theta(t - \tau) \sum_{n=1}^{N} [a_n + b_n(t - \tau)] e^{-\alpha_n(t-\tau)} \tag{2}$$

with order N, τ, a_n, b_n unknown and α_n predefined [5]. Differently from literature the solution is constrained via quadratic programming to $R^{DCB}(t_m) \geq 0 \forall t_m \in [t_1, t_{M-1}]$, and $R(t_M) = 0$. $N = 6$ was found sufficient.

For the CPI-based deconvolution we extend CPI+GDK [4] by substituting the VTF model with an exponential (EDK) and a lognormal (LNDK) kernels which are often considered in literature

$$\begin{cases} EDK(t) & = \frac{1}{\theta} e^{-\frac{1}{\theta}} \\ LNDK(t) & = \frac{1}{t\sigma\sqrt{2\pi}} e^{-\frac{(\ln(t)-\mu)^2}{2\sigma^2}} \end{cases} \tag{3}$$

where θ, μ, σ are unknowns. The CPI+GDK was implemented as in literature [4] with 12 control points and initial parameters p, s for the optimization routine $log2 \pm 2$ (*mean±SD*). Similarly the CPI+EDK and CPI+LNDK were initialized with $\theta = 1s \pm 2s$ and $\mu = -1 \pm 1, \sigma = 1 \pm 1$, which corresponds to low dispersion [4]. Non-linear estimation was peformed bounding parameters to $mean \pm 3SD$. We then proceed with two steps.

1. We perform synthetic experiments showing that DCB deconvolution performs comparably or better than CPI+GDK/EDK/LNDK when the ground truth dispersion kernel is GDK, EDK or LNDK respectively. Data was generated according to literature [2, 5] with $SNR = 50$ [4]. We tested three dispersion levels [4] low, medium, high, $BF \in [5 : 10 : 65]ml/100g/min$, $MTT \in [2 : 4 : 18]s$, delay $\in [0, 5]s$ (100 repetitions for each combination).

2. We apply DCB deconvolution on stroke MRI data to obtain the estimated $R^{eff}_{DCB}(t)$ for each voxel; we calculate the re-convolution $C^*_{ts}(t) = C_a \otimes R^{eff}_{DCB}(t)$; we perform deconvolution with the three CPI+ techniques on $C_a(t)$ and $C^*_{ts}(t)$ obtaining $R^{eff}_{GDK}(t)$, $R^{eff}_{EDK}(t)$ and $R^{eff}_{LNDK}(t)$; for each voxel we select the CPI+ technique scores the lowest l_2 reconstruction error of $C^*_{ts}(t)$, and the best estimates of the effective blood flow BF^{eff} and mean transit time MTT^{eff} using DCB results as a reference.

Results. Synthetic results in Fig. 1 show the comparisons of DCB with CPI+GDK/EDK/LNDK when the dispersion kernels are respectively GDK, EDK and LNDK. We note that MTT^{eff}, BF^{eff} estimates with DCB have lower or similar relative error. Results on real data in Fig. 2 show the clustering of a slice where each pixel is colored according to the CPI+ technique that better reproduces the $MTT^{eff}_{DCB}, BF^{eff}_{DCB}$ obtained with DCB, and the l_2 reconstruction error. Fig. 3 reports the BF^{eff} DCB-based map, which unveils an infarcted region in the right hemisphere.

Discussion. In-vivo results show that the presence of the GDK, EDK, LNDK dispersion kernels is widespread in the brain. Each clustered region looks structured and remains homogeneous among the tested parameters (see Fig. 2 "all"). We note that LNDK is more present in white matter, EDK in gray matter and GDK overlaps with the infarcted region as shown in Fig. 3 (see MTT^{eff} in Fig. 2 for instance). Synthetic results show that DCB allows performing reliable deconvolution without assumptions on the shape of VTF. At the same time the use of DCB opens for *a posteriori* VTF characterization, for instance with the three CPI+ based techniques.

Conclusion. We present results suggesting that different brain regions and tissue conditions support different descriptions of the underlying dispersion kernel (VTF), highlighting the need of estimating the effective residue amount of tracer $R^{eff}(t)$ with no *a priori* assumptions on the VTF, that is the case of DCB deconvolution. We further believe that successive dispersion kernel detection and characterization based on VTF models can constitute a new biomarker to shed light on the tissue vascular dynamic.

---

[1] Université Côte d'Azur, Inria, France; [†] expresses his thanks to Olea Medical and to the Provence-Alpes-Côte d'Azur Regional Council for providing support.
[2] Olea Medical, La Ciotat, France

References

[1] Willats et al., Improved deconvolution of perfusion mri data in the presence of bolus delay and dispersion, Magn Reson Med, vol. 56, pp. 146–156, 2006.

[2] Calamante et al., Delay and dispersion effects in dynamic susceptibility contrast mri: simulations using singular value decomposition, Magn Reson Med, vol. 44(3), pp. 466–473, 2000

[3] Calamante et al., Estimation of bolus dispersion effects in perfusion mri using image-based computational fluid dynamics, NeuroImage, vol. 19, pp. 341–353, 2003.

[4] Mehndiratta et al., Modeling and correction of bolus dispersion effects in dynamic susceptibility contrast mri: Dispersion correction with cpi in dsc-mri, Magn Reson Med, vol. 72, pp. 1762–1774, 2013.

[5] Pizzolato et al., Perfusion mri deconvolution with delay estimation and non-negativity constraints, in 12th International Symposium on Biomedical Imaging (ISBI). IEEE, 2015, pp. 1073–1076.
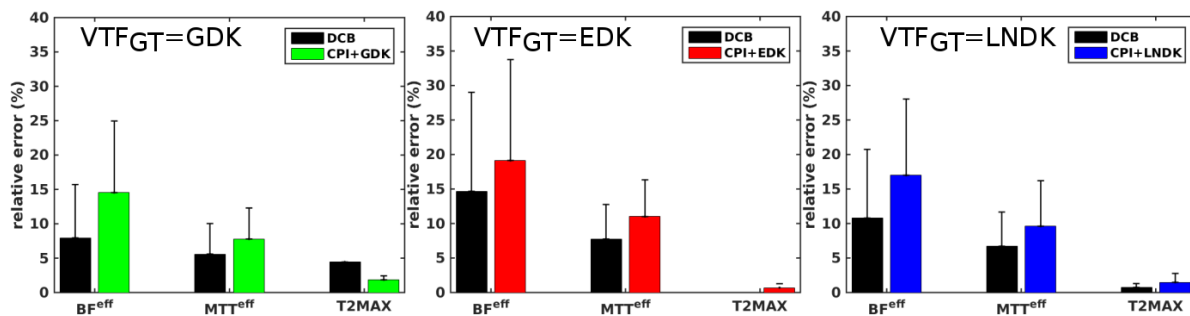
Figures

Figure 1: Relative errors $(mean, sd)$ of estimates of effective blood flow BF^{eff} calculated as the peak of the response function containing $R^{eff}(t)$, and mean transit time calculated as the ratio $MTT^{eff} = BV/BF^{eff}$ where BV is the computed blood volume [5]. Error in estimating the time-distance between the beginning of $R^{eff}(t)$ and its peak, $T2MAX$ is also reported.
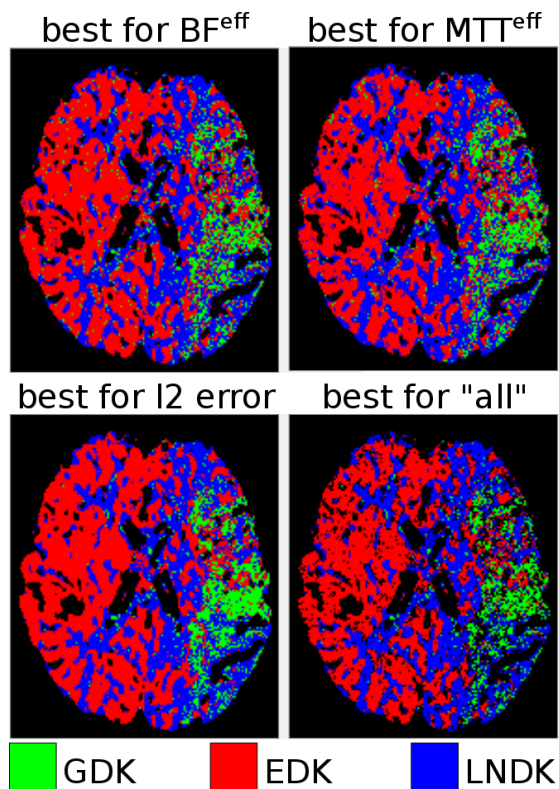

Figure 2: Best dispersion kernel based on DCB deconvolution. For each parameter, among BF^{eff}, MTT^{eff} and l_2 error, a pixel is colored according to the model-based technique that better describes DCB results among CPI+GDK [4] (green), CPI+EDK (red) and CPI+LNDK (blue). The "all" map shows the intersection of the results.
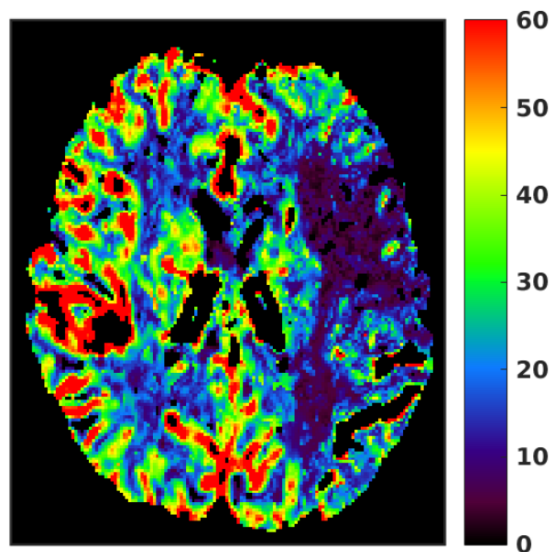

Figure 3: Effective cerebral blood flow BFeff (ml/100g/min) calculated from deconvolution by means of Dispersion-Compliant Bases [5] (DCB) on stroke MRI data. The right hemisphere shows an infarcted region characterized by low values whereas the surrounding tissue is iso-perfused. We note that the infarcted region visually correlates with GDK results in Fig. 2.